

Time Correlation and Variability of GeV Gamma-ray and X-ray emission from Active Galactic Nuclei

Kenji Nakagawa, Yoshihiro Umeda, and Masaki Mori

Department of Physical Sciences, Ritsumeikan University, Kusatsu, 525-8577 Shiga, Japan

Introduction

The LAT detector onboard the *Fermi* Gamma-ray Space Telescope and the *MAXI* detector onboard the International Space Station are monitoring the whole sky simultaneously at GeV gamma-ray and X-ray energies, respectively. Light curves of active galactic nuclei (AGN) have been accumulating with their data and are available on-line. These are the most contiguous datasets ever and the ideal database for time variation study in time scales of days and longer. In this paper we report the study of time correlation between GeV gamma-ray and X-ray emission and characteristic variability from some flaring AGN.

Data Set

Object names, observing periods and energy ranges used in this study are listed below.

Object	Detector	Observing Period [MJD]	Energy Range
3C273	Fermi LAT	54600-55800	100MeV-300GeV
	MAXI	55057-55631	1.5-20keV
3C454.3	Fermi LAT	54600-55800	100MeV-300GeV
	MAXI	55057-55622	1.5-20keV

Fermi LAT : <http://fermi.gsfc.nasa.gov/ssc/>

MAXI : <http://maxi.riken.jp/top/>

Analysis

Correlation Function

The correlation function in order to study correlation between Fermi LAT and MAXI observation data are defined as

$$CF(\tau) = \frac{E\{[a(t) - \bar{a}][b(t+\tau) - \bar{b}]\}}{\sigma_a \sigma_b} \quad (\text{Edelson and Krolik 1988})$$

where $E\{f\}$ is the expectation value of the function f , $a(t)$ and $b(t)$ is statistically stationary stochastic function. Barred variables are their mean, σ is its standard deviation.

Discrete Correlation Function

It is well known that correlated errors can lead to spurious contributions to the cross-correlation function at zero lag. To remedy these the use of the Discrete Correlation Function (DCF) has been suggested:

$$DCF(\tau) = \frac{(a_i - \bar{a})(b_j - \bar{b})}{M \sqrt{(\sigma_a^2 - e_a^2)(\sigma_b^2 - e_b^2)}} \quad (\text{Edelson and Krolik 1988})$$

where a_j and b_j are fluxes observed by Fermi LAT and MAXI, respectively. Barred variables are their mean, σ is its standard deviation, M is the number of data, and e_i is the measurement error associated with the data set f .

Power Spectrum Density

Power Spectrum Density analysis is the most common technique used to characterize the variability of the system. To reduce the effects caused by time lag between orbital periods of Fermi LAT and MAXI, we define the NPSD (normalized power spectrum density) as

$$P(f) = \frac{(a^2(f) + b^2(f) - \sigma_{\text{stat}}^2/n)T}{F_{\text{av}}^2}$$

$$a(f) = \frac{1}{n} \sum_{j=0}^{n-1} F_j \cos(2\pi f t_j) \quad b(f) = \frac{1}{n} \sum_{j=0}^{n-1} F_j \sin(2\pi f t_j)$$

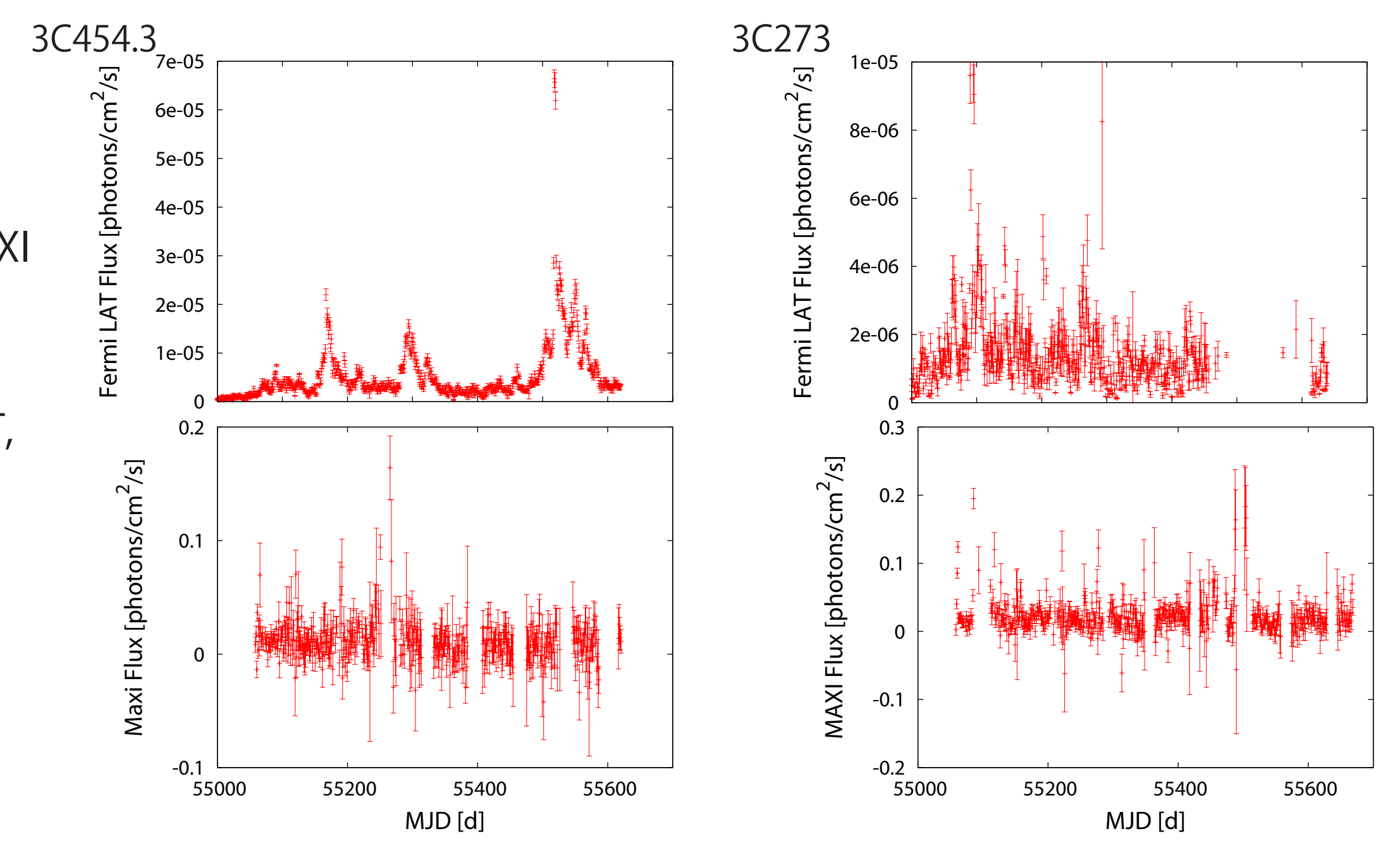
(Kataoka et al. 2001)

where f is the frequency, n is the number of data. F_j is the source count rate at time t_j ($0 \leq j \leq n-1$), T is the data length of the time series, and F_{av} is the mean value of the source counting rate.

Results

Light Curves

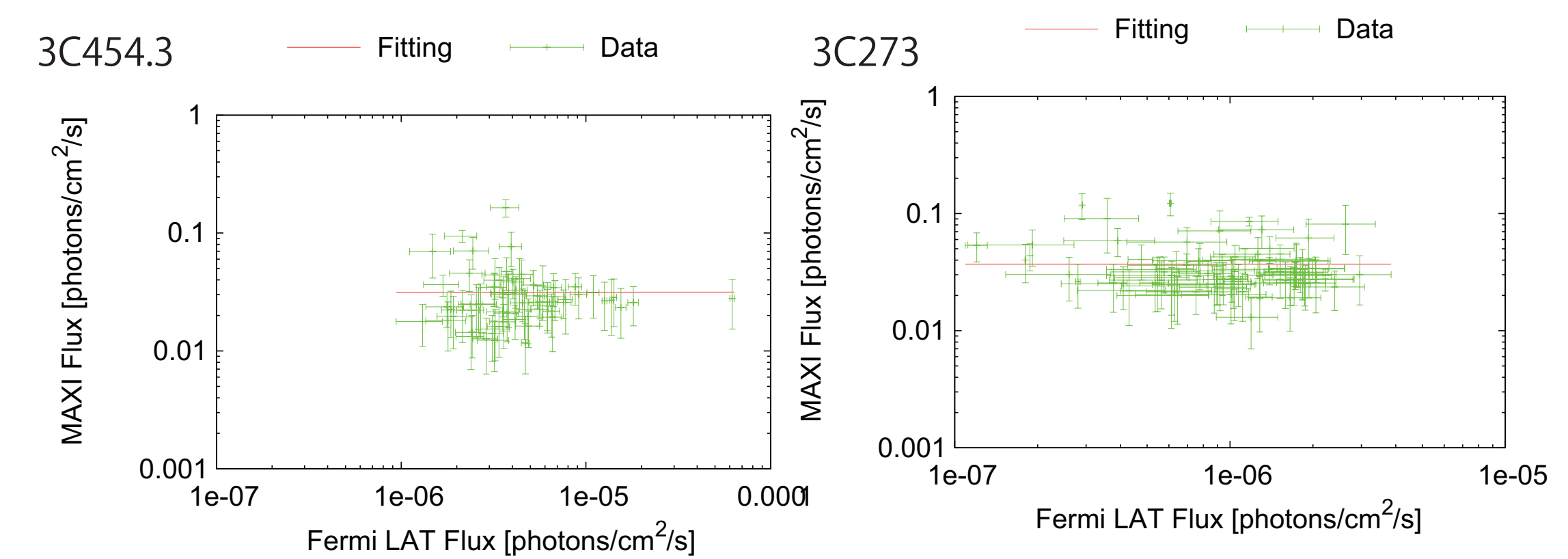
The daily light curves of Fermi LAT and MAXI for 3C454.3 and 3C273 during the whole period. Upper panels are the light curves of GeV gamma-rays observed by Fermi LAT, and the lower panels are those of X-rays by MAXI. The vertical axis is flux, and the horizontal axis is MJD.



Flux Correlation

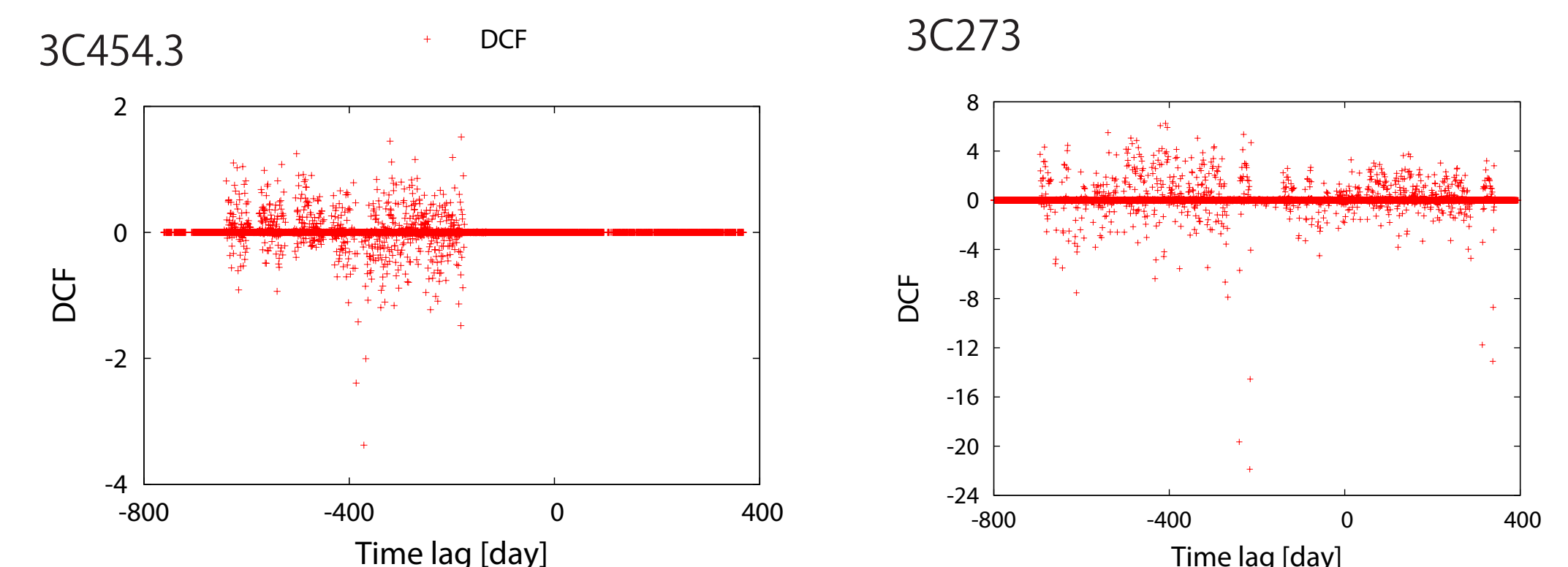
We associated Fermi LAT and MAXI fluxes with time lag within half day and computed correlation coefficients. The right figures are scatter plots of MAXI fluxes versus Fermi LAT fluxes for 3C454.3 and 3C273.

source	Correlation coefficient
3C454.3	-0.04
3C273	-0.18



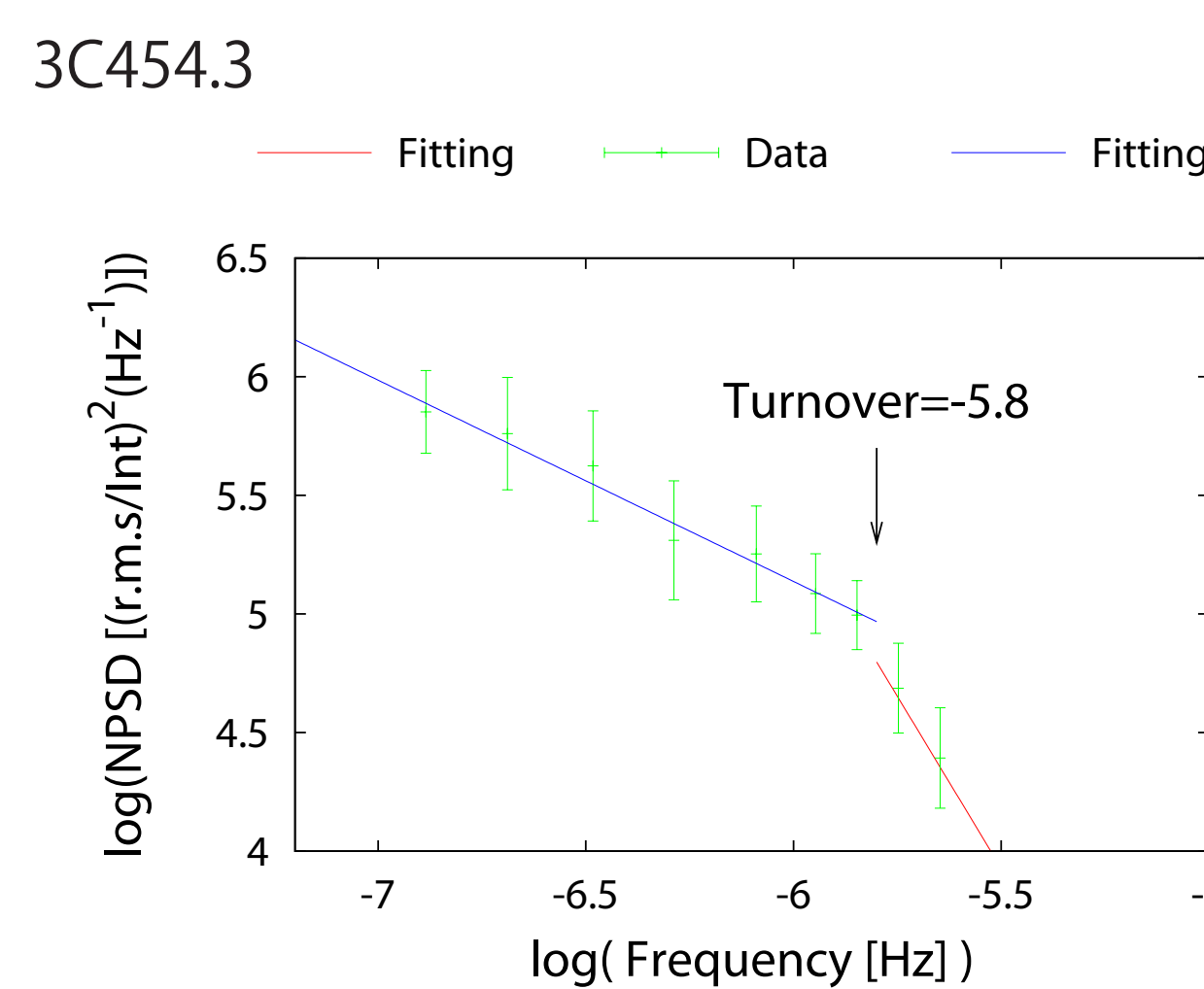
DCF

DCF (Discrete Correlation Function) is plotted as a function of time lag between Fermi LAT and MAXI observation time. The time lag is defined by $\Delta t = t_{\text{Fermi}} - t_{\text{MAXI}}$. We eliminate the term with $i=j$ to reduce correlation error.

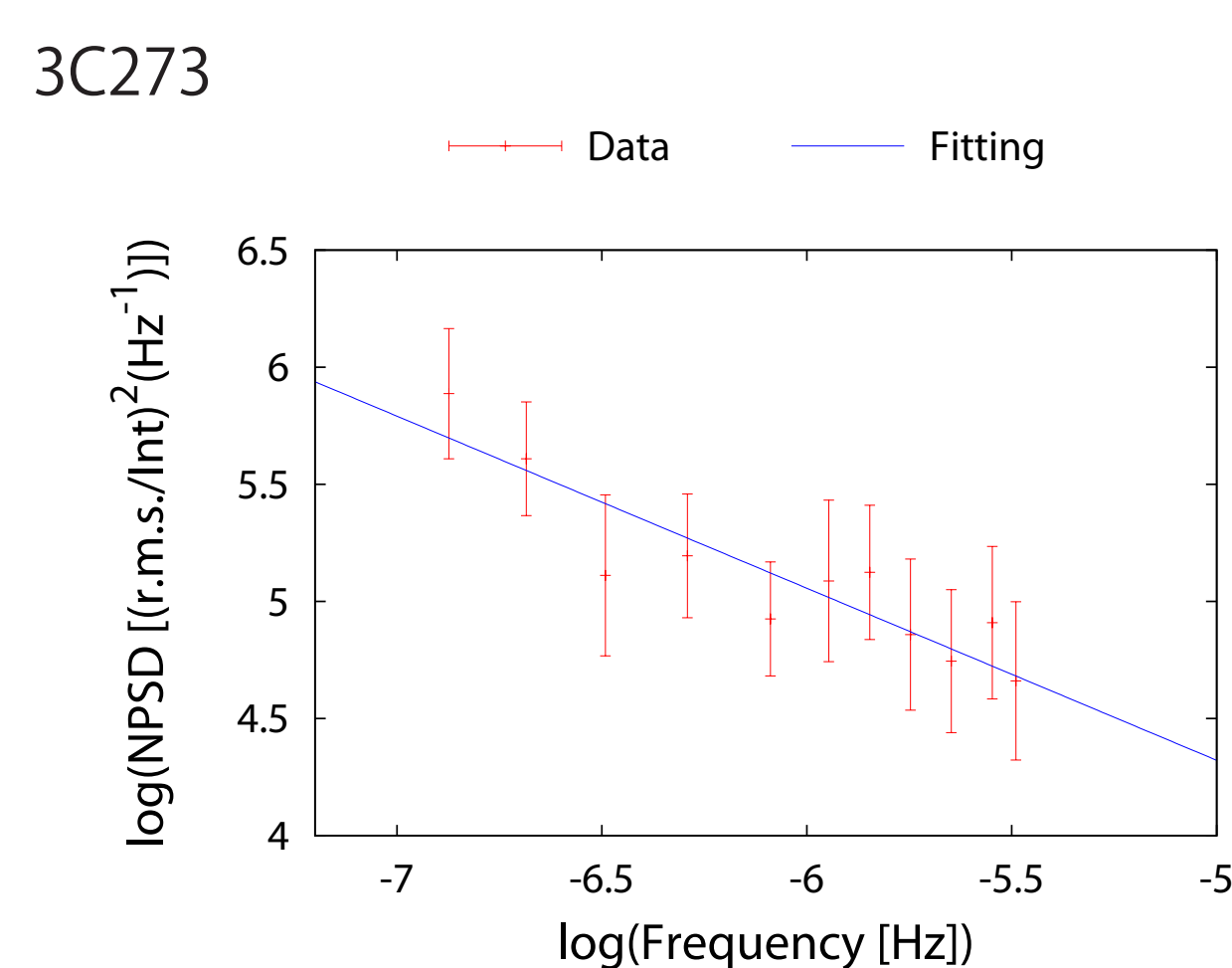


NPSD

The result of NPSD (normalized power spectrum density) analysis is as follows. In the left figures, the logarithmic horizontal axis is frequency and the vertical axis is NPSD, respectively. The right table is the result of fitting as a linear function, $y = ax + b$, assuming a turnover. (Red figures in the table are the parameters used in the linear fit in the plot.)



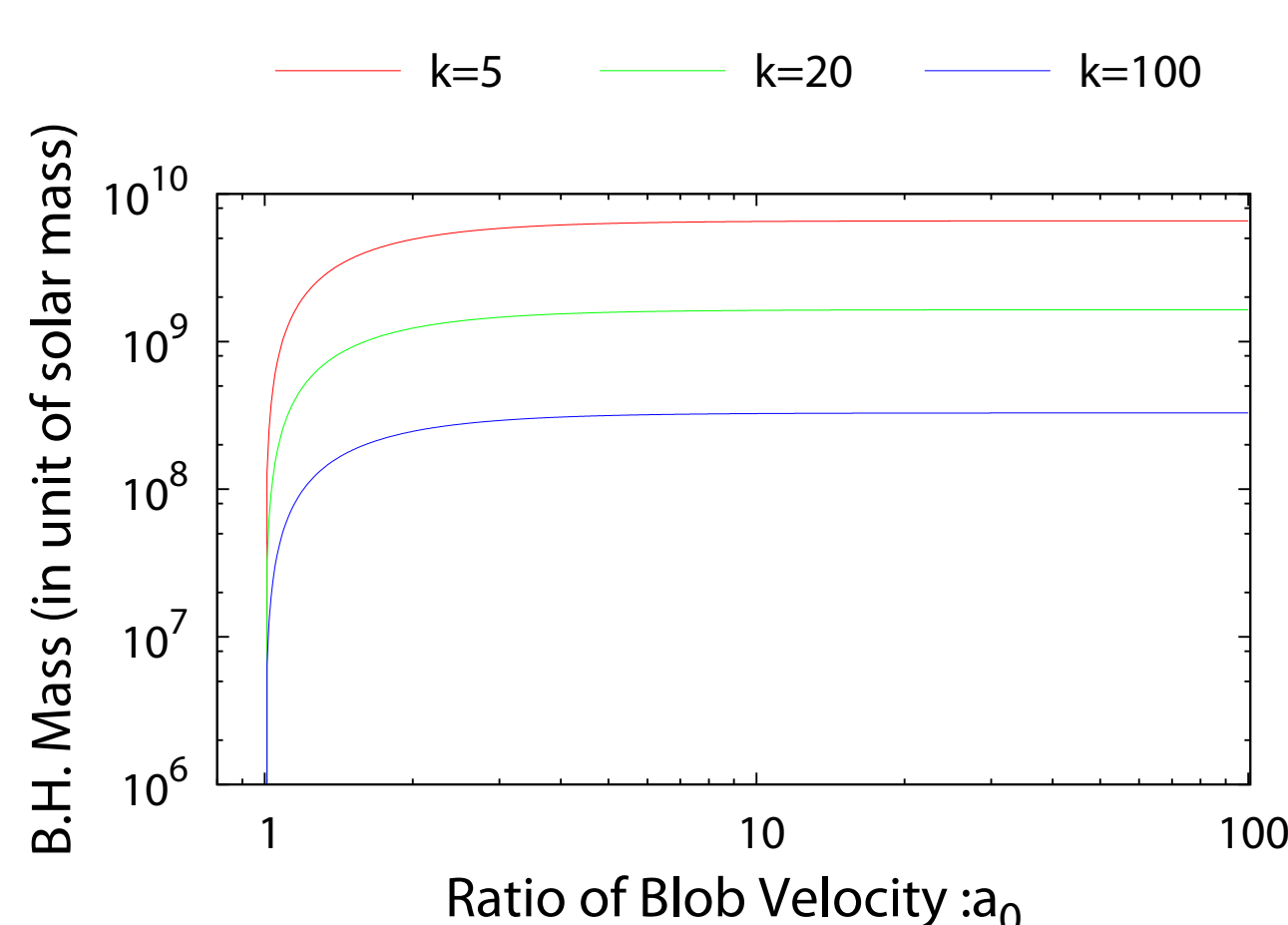
Turnover	a (>Turnover)	b (>Turnover)	a (<Turnover)	b (<Turnover)	χ^2
-5.6	-1.23	-2.97	-1.03	-1.12	0.99
-5.7	-2.57	-10.24	-0.93	-0.49	0.81
-5.8	-2.90	-12.02	-0.85	4.57	0.67
-5.9	-3.03	-12.27	-0.83	0.16	0.69
-6.0	-2.76	-11.24	-0.80	0.39	0.78



Turnover	a (>Turnover)	b (>Turnover)	a (<Turnover)	b (<Turnover)	χ^2
-	-0.73	0.65	-	-	0.84
-5.6	-0.79	0.28	-4.31	-19.03	0.72
-5.7	-0.79	0.29	-0.21	3.61	0.81
-5.8	-0.80	0.20	-0.38	2.66	0.81
-5.9	-1.00	-1.09	-0.98	-0.69	0.62

* χ^2 was not minimum, but there is no obvious turnover.

Discussion & Conclusion



There is no clear correlation between Fermi LAT and MAXI fluxes in this observation period. In addition, there is no characteristic time scale in the DCF analysis. PSD analysis of 3C454.3 shows a turnover around $10^{-5.8}$ Hz. We consider the mass of the central black hole with this result, following Kataoka et al. (2001). For simplicity, two relativistic blobs with bulk Lorentz factors Γ and $a_0\Gamma$ ejected at times $t=0$ and $t=\tau_0>0$, respectively. The faster blob will eventually catch up and collide with the first, slower blob, leading to shock formation and generation of a corresponding flare. In this case, taking the typical observed value, we can indicate by

$$M \simeq 9 \times 10^8 \frac{t_{\text{var}}}{\text{day}} \frac{10}{k} \frac{a_0^2 - 1}{2a_0^2} M_{\odot} \quad (\text{Kataoka et al. 2001})$$

Where $k \geq 3$. We plot the mass of the central black hole as a function of a_0 based on the result of PSD analysis of 3C454.3 (left figure). Here t_{var} is assumed to be the inverse of the turnover frequency: $t_{\text{var}} = 1.0/10^{\text{Turnover}} = 10^{5.8}$ [s]. Therefore, if the mass of the central black hole of 3C454.3 is

$$M_{3C454.3} \simeq 10^{8-10} M_{\odot}$$

the observational variability can be consistently explained.

Reference

1. Kataoka et al. 2001, ApJ, 560, 659-674
2. R.A. Edelson & J.H. Krolik 1988, ApJ, 333, 646-659